

Nanoscale Conducting and Insulating Domains on YbB₆

Aaron Coe,¹ Zhi-Huai Zhu,¹ Yang He,¹ Dae-Jeong Kim,²
Zachary Fisk,² Jason D. Hoffman,¹ and Jennifer E. Hoffman^{1,3,*}

¹*Department of Physics, Harvard University, Cambridge, MA, 02138, USA*

²*Department of Physics and Astronomy, University of California, Irvine, CA 92697, USA*

³*School of Engineering and Applied Science, Harvard University, Cambridge, MA, 02138, USA*

(Dated: January 22, 2024)

YbB₆ is a predicted topological insulator, with experimental evidence for conducting surface states of yet-unproven origin. However, its lack of a natural cleavage plane, and resultant surface-dependent polarity, has obscured its study. We use scanning tunneling microscopy to image the cleaved surface of YbB₆, exhibiting several coexisting terminations with distinct atomic structures. Our spectroscopic measurements show band-bending between the terminations, resulting in both conducting and fully-gapped regions. In the conductive regions, we observe spectral peaks that are suggestive of van Hove singularities arising from Rashba spin-split quantum well states. The insulating regions rule out the possibility that YbB₆ is a strong topological insulator, while the spin-polarized conducting regions suggest possible utility for spintronic devices.

Rare-earth hexaborides host a diverse set of exotic properties, ranging from superconductivity to magnetism to non-trivial topology. Interest in hexaborides surged when SmB₆ was predicted to be the first of a new type of correlated electron system, termed a topological Kondo insulator (TKI), in which protected surface states span a Kondo gap pinned around the Fermi level (E_F) [1, 2]. Extensive experiments, including transport [3–10], angle-resolved photoemission spectroscopy (ARPES) [11–18] and scanning tunneling microscopy/spectroscopy (STM/STS) [19, 20], demonstrated the existence of two-dimensional (2D) metallic surface states on SmB₆ at low temperatures. However, the topological nature of these states was unclear due to the multiple atomic terminations with complicated polar structure [15, 19–21]. Recently, quasiparticle interference (QPI) measurements on homogeneous terminations of SmB₆ revealed the heavy Dirac surface states within the Kondo gap [21, 22], establishing SmB₆ as the first TKI.

YbB₆, a second TKI candidate, was predicted to host a mixed valence of Yb around 2.2+, inverted Yb 4*f* and 5*d* bands, and topological surface states similar to SmB₆ [23]. Indeed, ARPES studies showed an odd number of Fermi pockets on the (001) cleaved surface of YbB₆ [24–27], with the chirality of orbital angular momentum [24], spin texture [25], and temperature and photon energy dependence [26] expected for topological surface states. Quantum oscillation measurements confirmed consistent surface Fermi pocket areas [28, 29]. However, magnetic susceptibility [30], optical reflectivity [31], and x-ray and ultraviolet photoemission [32] showed that Yb is uniformly divalent in the bulk of YbB₆, with a modest Yb³⁺ fraction only at the surface. Furthermore, the highest occupied Yb 4*f* state was consistently found around 1 eV below E_F [24–27, 32], ruling out the TKI scenario, and requiring an alternate explanation for the surface states.

Two distinct mechanisms for the YbB₆ surface states have been proposed. The first claims strong topological surface states originating from inversion of the bulk Yb 5*d* and B 2*p* bands [26, 33], as schematized in Fig. 1(a). The second claims trivial quantum well states due to band-bending at the polar (001) surface of YbB₆ [34, 35], as schematized in Fig. 1(b). The latter proposal is supported by the parabolic dispersion of (001) surface states [27], and additional ARPES measurements on the non-polar (110) surface showing a robust ~ 0.3 eV gap between the B 2*p* valence and Yb 5*d* conduction bands [34]. Each proposal is supported by density functional theory (DFT) calculations with minor parameter variations. However, neither proposal appears fully consistent with all experimental data. All ARPES and quantum oscillation experiments on both (001) and (110) surfaces showed conducting states, despite the various *p*-type, *n*-type, and non-polar terminations expected. Yet no surface channel was seen in magnetoresistance measurements [7]. Given the likelihood of spectral artifacts from these existing experiments that spatially average over different terminations [21], it remains crucial to conduct local imaging experiments to distinguish between proposals by spatially correlating surface spectral features with specific terminations.

Here, we use STM/STS to demonstrate termination-dependent surface conductivity in YbB₆. Our spatially-resolved differential conductance spectra (dI/dV) show strong band bending associated with surface polarity, leading to coexisting insulating and conducting domains. The observation of insulating domains on clean regions of YbB₆ definitively rules out the possibility of a strong topological insulator state. Within the conducting domains, we observe multiple in-gap peaks reminiscent of van Hove singularities that may stem from Rashba spin-split quantum well states, schematized in Fig. 1(c).

Single crystals of YbB₆ were grown by the Al-flux method [7], cleaved in ultra-high vacuum (UHV) at cryogenic temperatures, and immediately inserted into a home-built STM at 4.2 K. YbB₆, possessing a CsCl-

* jhoffman@physics.harvard.edu

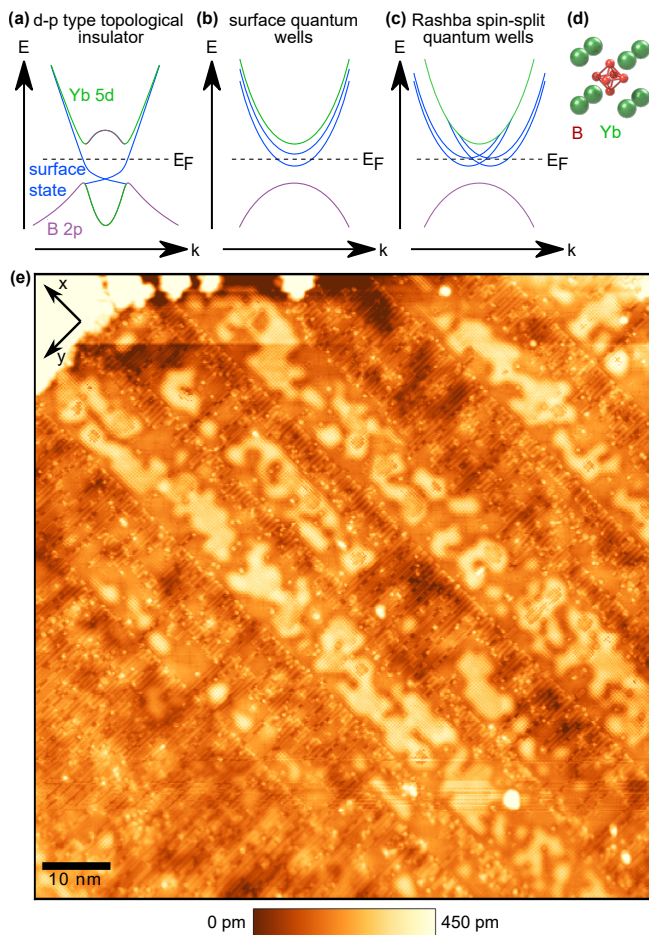


FIG. 1. (a) Topological insulator, (b) quantum wells, and (c) Rashba spin-split quantum wells band structure proposals. (d) CsCl crystal structure of YbB_6 . (e) STM topographic image, showing multiple terminations on cleaved YbB_6 (sample bias $V_s = -0.15$ V; current setpoint $I_s = 100$ pA). Values on the color bar indicate apparent height and not actual height due to the polar surface effects in YbB_6 .

type crystal structure shown in Fig. 1(d), does not have a natural cleavage plane. Because the intra- and inter-octahedral B-B bonds have similar lengths [36], several terminations are possible by breaking both types of bonds. Breaking inter-octahedral bonds results in the B_6 and Yb terminations. Alternatively, breaking intra-octahedral bonds can lead to disordered and inhomogeneous terminations with incomplete B octahedra. In our STM study, we find the surface morphology of cleaved YbB_6 exhibits both 1×1 and chain domains, arranged in alternating strips along the $[100]$ crystal axis, as shown in Fig. 1(e). In the 1×1 domains [Fig. 2(a,c)], we measured an atomic spacing consistent with the expected YbB_6 lattice constant of $a = 4.1439$ Å [36–38]. In the chain domains [Fig. 2(b,d)], the inter-chain period is exactly doubled.

Average dI/dV spectra from each domain, which represent the local density of states (DOS), are shown in

Fig. 2(e). Both spectra exhibit a large range of reduced DOS around E_F , and prominent peaks at negative bias, which we identify as the Yb^{2+} $4f$ multiplets. These $4f$ states are often observed by spatially-averaged APRES experiments around -1 eV and -2.3 eV [24–27], though energies may vary by up to 500 meV between samples [24] and time after cleaving [27]. The chain domain spectra exhibit an additional rise at positive bias, which may be identified as a broad Yb $5d$ band, as observed by inverse photoemission [31]. The energy shift between our dI/dV spectra suggests terminations with different surface polarities, as commonly observed via spatially-resolved measurements on other semiconductors [21, 39]. On cleaved YbB_6 , we expect that a Yb-terminated surface would be positively charged compared to the bulk because the B octahedra take electrons from the Yb layer to form their bonds. Bulk free electrons then move towards the surface to screen the positive surface electrostatic potential, forming an accumulation layer with excess electrons (n -type), and inducing a downward band-bending. Similarly, we expect that a B_6 -terminated surface would be negatively charged, giving rise to a p -type environment and upward band-bending. However, not all B-terminated surfaces need be negatively charged; e.g., the B_1 termination requires fewer electrons from the Yb layers to form the octahedral bonds.

In the dI/dV spectra of Fig. 2(e), the low-conductance energy range around E_F on the chain domain is smaller than that on the 1×1 domain. The change in energy range can be explained by a combination of tip-induced band bending (TIBB), polar surface band bending, and the presence of in-gap surface states. STM measurements of insulator gap amplitudes are known to vary from their intrinsic values as a result of poor electronic screening, which allows the electric field generated by the tip to partially penetrate the sample surface [40]. For semiconductors with polar surfaces, tip-induced bending of the bulk bands at the surface can lead to apparent variations in gap amplitude and shifts of the gap between different surfaces [39]. YbB_6 is subject to both band-bending effects, in addition to in-gap states that can alter the electronic screening and thus the overall energy separation.

Combining topographic and spectroscopic data, we can identify the two observed terminations. The upward band shift of the 1×1 domain tells us that it must possess a greater number of negatively-charged B atoms with respect to the chain domain, so it cannot represent a Yb termination. Due to its clean structure and atomic periodicity, we infer that the 1×1 domain is either the B_1 or B_6 termination. In contrast, the double periodicity of the chains tells us that it is a partial layer termination. Furthermore, the chains are laterally offset from the 1×1 atoms, as highlighted in Fig. 3(a), where blue lines indicate the chain centers and red dots indicate the top B atoms of each octahedron. Averaged linecuts for the chain and 1×1 domains are shown in Fig. 3(b). We can therefore rule out a partial Yb termination as the chain domain identity, because Yb chains would terminate di-

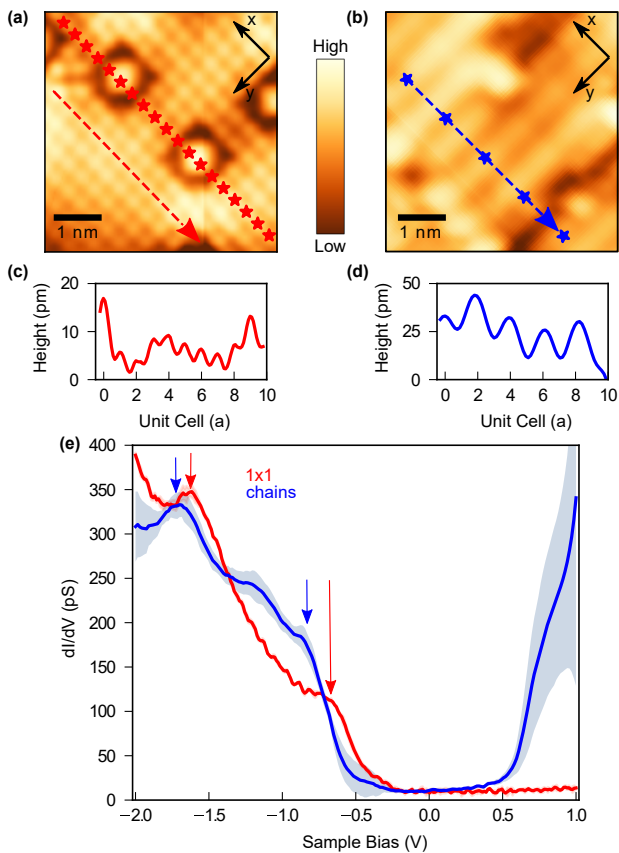


FIG. 2. (a, b) High resolution topographies of YbB_6 (001) surface showing two distinct terminations: (a) 1×1 domain ($V_s = -0.4$ V, $I_s = 200$ pA) and (b) chain domain ($V_s = 0.2$ V, $I_s = 100$ pA). (c, d) Linecuts along respective dashed lines, calibrated to the cryogenic temperature adjusted YbB_6 lattice constant $a = 4.1439$ Å [36, 37]. (e) dI/dV spectra averaged over the starred locations in (a) and (b), with shaded standard deviation ($V_s = -2$ V, $I_s = 400$ pA, lockin modulation $V_{\text{rms}} = 15$ mV).

rectly between 1×1 B_1 or B_6 surface atoms. Therefore, the chains can be identified as a partial B termination. Due to the up-shifted spectra, we know that the 1×1 domain must have more B atoms than the chain domain, so we conclude that the 1×1 domain must be B_6 rather than B_1 . The proposed crystal structure for the 1×1 domain and an example B_4 termination for the chain domain are illustrated in Fig. 3(c,d), respectively. Other possibilities for the chain domain include tilted B_6 octahedra, or B_5 , B_3 , and B_2 terminations.

To understand the YbB_6 surface states previously observed by spatially-averaging probes [24–29], we zoom in on the near- E_F states that are swamped by the dominant $4f$ multiplets in Fig. 2(e). Figure 4 shows a topography and dI/dV map of the same area over a smaller energy range around E_F , acquired with lower junction resistance for increased sensitivity to sub-gap features. With this increased sensitivity, we observe a true insulating gap on $\sim 25\%$ of the surface, corresponding to clean 1×1 regions

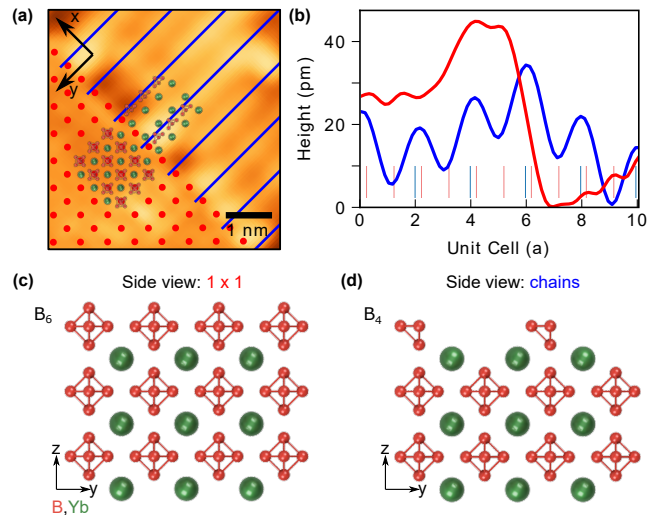


FIG. 3. (a) Topography showing a boundary between 1×1 and chain regions ($V_s = 0.2$ V, $I_s = 100$ pA). The blue lines are along the centers of the chains and the red points correspond to the individual atoms on the 1×1 surface. (b) Averaged linecuts across 1×1 and chain domains in (a). Vertical lines represent the unit cell spacing for each surface. (c, d) Side view of the B_6 and B_4 surface terminations, respectively.

in Fig. 4(a), and depicted in a black-red colorscale in Fig. 4(b). The average spectra from these regions are shown in corresponding colors in Fig. 4(c), with apparent gap amplitude ~ 100 meV roughly consistent with the known bulk gap [30]. We caution that TIBB is likely even more significant at this lower junction resistance where the tip is closer to the sample, but we emphasize that TIBB cannot create an apparent gap, though it can change an existing gap amplitude. Therefore, the $\sim 25\%$ gapped area definitively rules out a strong topological surface state, which would necessarily cover all surfaces [41, 42].

The remaining $\sim 75\%$ of the YbB_6 surface, comprising most of the chain domains and a smaller fraction of the 1×1 domains, shows in-gap states with one or two peaks at energies near E_F . The average spectra, binned by their minimum in-gap peak energy, are shown in Fig. 4(c). Though YbB_6 is a bulk insulator [30], the demonstrated surface polarity may bend a bulk band to cross E_F at the surface. Confinement within a few nanometers of the surface reduces the 3-dimensional band to a discrete number of 2-dimensional bands known as quantum well states (QWS), as suggested by previous ARPES experiments [27, 34], and schematized in Fig. 1(b). But these QWS alone would not give rise to a peak in the density of states. To explain our observed peak, as well as the spin-polarization measured by ARPES [25], we suggest that Rashba spin-orbit coupling (SOC) splits the surface bands, as schematized in Fig. 1(c). The spin-splitting would give rise to a van Hove singularity (vHS) and observable peak in the density of states at the minimum energy of the QWS [39, 43]. The ~ 150 mV variation of sub-gap peak energy in Fig. 4(c) may be attributed

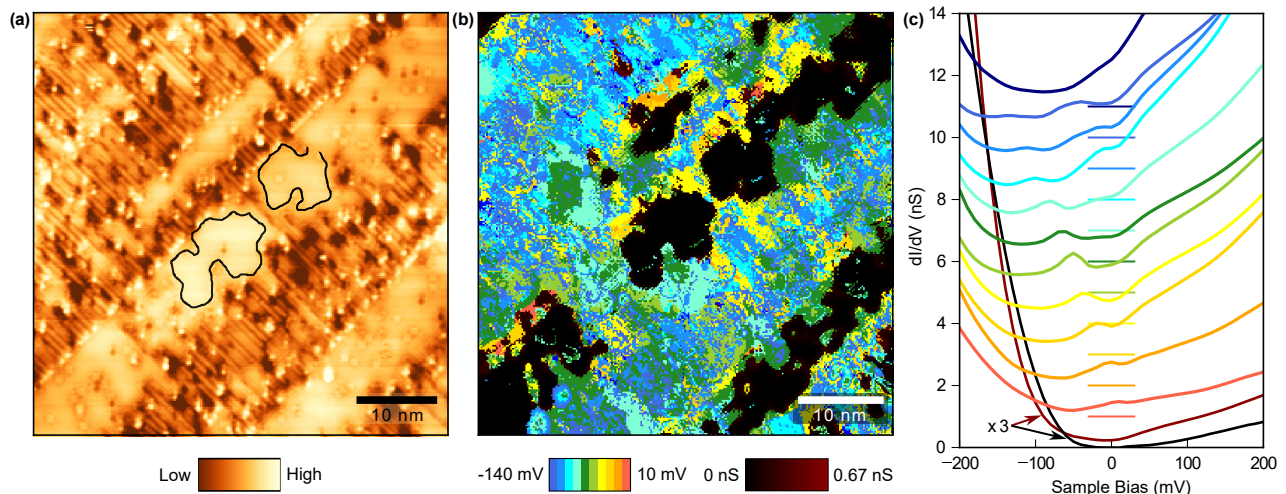


FIG. 4. (a) Surface topography, acquired in the same area immediately prior to the dI/dV map that is analyzed in (b,c) ($V_s = -1$ V, $I_s = 50$ pA, $V_{\text{rms}} = 15$ mV). (b) Map showing the presence (bright colors) or absence (dark colors) of in-gap states. The energy of the first in-gap peak from the valence band edge is depicted in a rainbow palette. Less than 1% of the surface exhibits in-gap states without a discernible peak, depicted in dark blue. Regions without detectable in-gap states are shown instead using a black-red palette depicting the tunneling conductance near E_F (averaged from -20 meV to $+20$ meV). (c) Averaged dI/dV spectra from (b) showing sub-gap peaks in the 10 color bins, each offset vertically by 1 nS with horizontal lines to represent their zero for clearer comparison. Close to 25% of the surface spectra show no in-gap states. These gapped spectra, averaged over regions with tunneling conductance below 1 pS (black) and above 1 pS (dark red) are shown with zero offset, but $3\times$ magnification to emphasize the true Fermi-level gap.

to band bending from the two surface terminations, and further local band bending from the many atomic-scale defects apparent in Fig. 4(a).

In conclusion, our STM/STS study provides the first real-space imaging of YbB_6 . On the (001) surface, we observe two different atomic terminations whose distinct polarity is evidenced by spectra shifts greater than 100 meV. Furthermore, we observe both conducting and insulating nanoscale domains, definitively ruling out the proposed strong topological surface state for YbB_6 . Instead, we show that the surface states previously observed by spatially-averaging techniques arise from quantum well states induced by surface band bending. We further show that the quantum well states are Rashba spin-split, evidenced by sub-gap peaks consistent with van Hove

singularities in the conductance spectra. The coexisting nanoscale domains with differing surface polarities suggests YbB_6 may represent a new class of strongly-correlated materials with utility for spin-polarized p - n junctions or other spintronic devices [39].

ACKNOWLEDGMENTS

We acknowledge Ruizhe Kang, Harry Pirie, Christian Matt, Can-Li Song, and Dennis Huang for helpful discussions. A.C. was funded by the Air Force Office of Scientific Research Multidisciplinary University Research Initiative through Award No. FA9550-21-1-0429.

-
- [1] M. Dzero, K. Sun, V. Galitski, and P. Coleman, Topological Kondo insulators, *Phys. Rev. Lett.* **104**, 106408 (2010).
 - [2] M. Dzero, K. Sun, P. Coleman, and V. Galitski, Theory of topological Kondo insulators, *Phys. Rev. B* **85**, 045130 (2012).
 - [3] S. Wolgast, Ç. Kurdak, K. Sun, J. W. Allen, D.-J. Kim, and Z. Fisk, Low-temperature surface conduction in the Kondo insulator SmB_6 , *Phys. Rev. B* **88**, 180405(R) (2013).
 - [4] X. Zhang, N. P. Butch, P. Syers, S. Ziemak, R. L. Greene, and J. Paglione, Hybridization, inter-ion correlation, and surface states in the Kondo insulator SmB_6 , *Phys. Rev. X* **3**, 011011 (2013).
 - [5] G. Li, Z. Xiang, F. Yu, T. Asaba, B. Lawson, P. Cai, C. Tinsman, A. Berkley, S. Wolgast, Y. S. Eo, D.-J. Kim, C. Kurdak, J. W. Allen, K. Sun, X. H. Chen, Y. Y. Wang, Z. Fisk, and L. Li, Two-dimensional Fermi surfaces in Kondo insulator SmB_6 , *Science* **346**, 1208 (2014).
 - [6] D. J. Kim, S. Thomas, T. Grant, J. Botimer, Z. Fisk, and J. Xia, Surface Hall effect and nonlocal transport in SmB_6 : Evidence for surface conduction, *Sci. Rep.* **3**, 3150 (2013).
 - [7] D. J. Kim, J. Xia, and Z. Fisk, Topological surface state in the Kondo insulator samarium hexaboride, *Nat. Mater.* **13**, 466 (2014).

- [8] Y. Nakajima, P. Syers, X. Wang, R. Wang, and J. Paglione, One-dimensional edge state transport in a topological Kondo insulator, *Nat. Phys.* **12**, 213 (2016).
- [9] W. A. Phelan, S. M. Koohpayeh, P. Cottingham, J. W. Freeland, J. C. Leiner, C. L. Broholm, and T. M. McQueen, Correlation between bulk thermodynamic measurements and the low-temperature-resistance plateau in SmB_6 , *Phys. Rev. X* **4**, 031012 (2014).
- [10] P. Syers, D. Kim, M. S. Fuhrer, and J. Paglione, Tuning bulk and surface conduction in the proposed topological Kondo insulator SmB_6 , *Phys. Rev. Lett.* **114**, 096601 (2015).
- [11] N. Xu, X. Shi, P. K. Biswas, C. E. Matt, R. S. Dhaka, Y. Huang, N. C. Plumb, M. Radović, J. H. Dil, E. Pomjakushina, K. Conder, A. Amato, Z. Salman, D. M. Paul, J. Mesot, H. Ding, and M. Shi, Surface and bulk electronic structure of the strongly correlated system SmB_6 and implications for a topological Kondo insulator, *Phys. Rev. B* **88**, 121102(R) (2013).
- [12] J. Jiang, S. Li, T. Zhang, Z. Sun, F. Chen, Z. R. Ye, M. Xu, Q. Q. Ge, S. Y. Tan, X. H. Niu, M. Xia, B. P. Xie, Y. F. Li, X. H. Chen, H. H. Wen, and D. L. Feng, Observation of possible topological in-gap surface states in the Kondo insulator SmB_6 by photoemission, *Nat. Commun.* **4**, 3010 (2013).
- [13] M. Neupane, N. Alidoust, S.-Y. Xu, T. Kondo, Y. Ishida, D. J. Kim, C. Liu, I. Belopolski, Y. J. Jo, T.-R. Chang, H.-T. Jeng, T. Durakiewicz, L. Balicas, H. Lin, A. Bansil, S. Shin, Z. Fisk, and M. Z. Hasan, Surface electronic structure of the topological Kondo-insulator candidate correlated electron system SmB_6 , *Nat. Commun.* **4**, 2991 (2013).
- [14] E. Frantzeskakis, N. de Jong, B. Zwartsenberg, Y. K. Huang, Y. Pan, X. Zhang, J. X. Zhang, F. X. Zhang, L. H. Bao, O. Tegus, A. Varykhalov, A. de Visser, and M. S. Golden, Kondo hybridization and the origin of metallic states at the (001) surface of SmB_6 , *Phys. Rev. X* **3**, 041024 (2013).
- [15] Z.-H. Zhu, A. Nicolaou, G. Levy, N. P. Butch, P. Syers, X. F. Wang, J. Paglione, G. A. Sawatzky, I. S. Elfimov, and A. Damascelli, Polarity-driven surface metallicity in SmB_6 , *Phys. Rev. Lett.* **111**, 216402 (2013).
- [16] J. D. Denlinger, J. W. Allen, J.-S. Kang, K. Sun, J.-W. Kim, J. H. Shim, B. I. Min, D.-J. Kim, and Z. Fisk, Temperature dependence of linked gap and surface state evolution in the mixed valent topological insulator SmB_6 , *arXiv:1312.6637 [cond-mat]* (2014).
- [17] C.-H. Min, P. Lutz, S. Fiedler, B. Y. Kang, B. K. Cho, H.-D. Kim, H. Bentmann, and F. Reinert, Importance of charge fluctuations for the topological phase in SmB_6 , *Phys. Rev. Lett.* **112**, 226402 (2014).
- [18] N. Xu, P. K. Biswas, J. H. Dil, R. S. Dhaka, G. Landolt, S. Muff, C. E. Matt, X. Shi, N. C. Plumb, M. Radović, E. Pomjakushina, K. Conder, A. Amato, S. V. Borisenko, R. Yu, H.-M. Weng, Z. Fang, X. Dai, J. Mesot, H. Ding, and M. Shi, Direct observation of the spin texture in SmB_6 as evidence of the topological Kondo insulator, *Nat. Commun.* **5**, 4566 (2014).
- [19] S. Rößler, T.-H. Jang, D.-J. Kim, L. H. Tjeng, Z. Fisk, F. Steglich, and S. Wirth, Hybridization gap and Fano resonance in SmB_6 , *PNAS* **111**, 4798 (2014).
- [20] W. Ruan, C. Ye, M. Guo, F. Chen, X. Chen, G.-M. Zhang, and Y. Wang, Emergence of a coherent in-gap state in the SmB_6 Kondo insulator revealed by scanning tunneling spectroscopy, *Phys. Rev. Lett.* **112**, 136401 (2014).
- [21] C. E. Matt, H. Pirie, A. Soumyanarayanan, Y. He, M. M. Yee, P. Chen, Y. Liu, D. T. Larson, W. S. Paz, J. J. Palacios, M. H. Hamidian, and J. E. Hoffman, Consistency between ARPES and STM measurements on SmB_6 , *Phys. Rev. B* **101**, 085142 (2020).
- [22] H. Pirie, Y. Liu, A. Soumyanarayanan, P. Chen, Y. He, M. M. Yee, P. F. S. Rosa, J. D. Thompson, D.-J. Kim, Z. Fisk, X. Wang, J. Paglione, D. K. Morr, M. H. Hamidian, and J. E. Hoffman, Imaging emergent heavy Dirac fermions of a topological Kondo insulator, *Nat. Phys.* **16**, 52 (2020).
- [23] H. Weng, J. Zhao, Z. Wang, Z. Fang, and X. Dai, Topological crystalline Kondo insulator in mixed valence ytterbium borides, *Phys. Rev. Lett.* **112**, 016403 (2014).
- [24] M. Xia, J. Jiang, Z. R. Ye, Y. H. Wang, Y. Zhang, S. D. Chen, X. H. Niu, D. F. Xu, F. Chen, X. H. Chen, B. P. Xie, T. Zhang, and D. L. Feng, Angle-resolved photoemission spectroscopy study on the surface states of the correlated topological insulator YbB_6 , *Sci. Rep.* **4**, 5999 (2014).
- [25] N. Xu, C. E. Matt, E. Pomjakushina, J. H. Dil, G. Landolt, J.-Z. Ma, X. Shi, R. S. Dhaka, N. C. Plumb, M. Radović, V. N. Strocov, T. K. Kim, M. Hoesch, K. Conder, J. Mesot, H. Ding, and M. Shi, Surface vs bulk electronic structures of a moderately correlated topological insulator YbB_6 revealed by ARPES, *arXiv:1405.0165 [cond-mat]* (2014).
- [26] M. Neupane, S.-Y. Xu, N. Alidoust, G. Bian, D. J. Kim, C. Liu, I. Belopolski, T.-R. Chang, H.-T. Jeng, T. Durakiewicz, H. Lin, A. Bansil, Z. Fisk, and M. Z. Hasan, Non-Kondo-like electronic structure in the correlated rare-earth hexaboride YbB_6 , *Phys. Rev. Lett.* **114**, 016403 (2015).
- [27] E. Frantzeskakis, N. de Jong, J. X. Zhang, X. Zhang, Z. Li, C. L. Liang, Y. Wang, A. Varykhalov, Y. K. Huang, and M. S. Golden, Insights from angle-resolved photoemission spectroscopy on the metallic states of $\text{YbB}_6(001):E(k)$ dispersion, temporal changes, and spatial variation, *Phys. Rev. B* **90**, 235116 (2014).
- [28] Z. Xiang, Y. Kasahara, T. Asaba, B. Lawson, C. Tinsman, L. Chen, K. Sugimoto, S. Kawaguchi, Y. Sato, G. Li, S. Yao, Y. L. Chen, F. Iga, J. Singleton, Y. Matsuda, and L. Li, Quantum oscillations of electrical resistivity in an insulator, *Science* **362**, 65 (2018).
- [29] T. Zhang, G. Li, S. C. Sun, N. Qin, L. Kang, S. H. Yao, H. M. Weng, S. K. Mo, L. Li, Z. K. Liu, L. X. Yang, and Y. L. Chen, Electronic structure of correlated topological insulator candidate YbB_6 studied by photoemission and quantum oscillation, *Chinese Physics B* **29**, 017304 (2020).
- [30] J. M. Tarascon, J. Etourneau, P. Dordor, P. Hagenmuller, M. Kasaya, and J. M. D. Coey, Magnetic and transport properties of pure and carbon-doped divalent RE hexaboride single crystals, *J. Appl. Phys.* **51**, 574 (1980).
- [31] T. Nanba, M. Tomikawa, Y. Mori, N. Shino, S. Imada, S. Suga, S. Kimura, and S. Kunii, Valency of YbB_6 , *Phys. B: Condens. Matter* **186-188**, 557 (1993).
- [32] A. Kakizaki, A. Harasawa, T. Kinoshita, T. Ishii, T. Nanba, and S. Kunii, XPS and UPS studies of the electronic structures of YbB_6 , *Phys. B: Condens. Matter* **186-188**, 80 (1993).
- [33] T.-R. Chang, T. Das, P.-J. Chen, M. Neupane, S.-Y. Xu,

- M. Z. Hasan, H. Lin, H.-T. Jeng, and A. Bansil, Two distinct topological phases in the mixed-valence compound YbB_6 and its differences from SmB_6 , *Phys. Rev. B* **91**, 155151 (2015).
- [34] C.-J. Kang, J. D. Denlinger, J. W. Allen, C.-H. Min, F. Reinert, B. Y. Kang, B. K. Cho, J.-S. Kang, J. H. Shim, and B. I. Min, Electronic structure of YbB_6 : Is it a topological insulator or not?, *Phys. Rev. Lett.* **116**, 116401 (2016).
- [35] S. Ramankutty, N. de Jong, Y. Huang, B. Zwartsenberg, F. Masee, T. Bay, M. Golden, and E. Frantzeskakis, Comparative study of rare earth hexaborides using high resolution angle-resolved photoemission, *Journal of Electron Spectroscopy and Related Phenomena* **208**, 43 (2016).
- [36] M. K. Blomberg, M. J. Merisalo, M. M. Korsukova, and V. N. Gurin, Single-crystal X-ray diffraction study of NbB_6 , EuB_6 and YbB_6 , *J. Alloys Compd.* **217**, 123 (1995).
- [37] J. Etourneau, J.-P. Mercurio, R. Naslain, and P. Hagemuller, Structure électronique de quelques hexaborures de type CaB_6 , *Journal of Solid State Chemistry* **2**, 332 (1970).
- [38] The expected YbB_6 lattice constant of $a = 4.1439 \text{ \AA}$ was inferred from the room-temperature value $a = 4.1479 \text{ \AA}$ measured by x-ray diffraction on single crystals of YbB_6 [36], and the thermal contraction of 0.096% from room temperature to 4 K, measured in other rare-earth hexaborides [37]. After verifying $\sim 5\%$ consistency with our independent rough calibration, all topographies are displayed with refined calibration using the exact value $a = 4.1439 \text{ \AA}$.
- [39] C. Tournier-Colletta, G. Autès, B. Kierren, P. Bugnon, H. Berger, Y. Fagot-Revurat, O. V. Yazyev, M. Grioni, and D. Malterre, Atomic and electronic structure of a Rashba $p - n$ junction at the BiTeI surface, *Phys. Rev. B* **89**, 085402 (2014).
- [40] I. Battisti, V. Fedoseev, K. M. Bastiaans, A. de la Torre, R. S. Perry, F. Baumberger, and M. P. Allan, Poor electronic screening in lightly doped Mott insulators observed with scanning tunneling microscopy, *Phys. Rev. B* **95**, 235141 (2017).
- [41] L. Fu, C. L. Kane, and E. J. Mele, Topological insulators in three dimensions, *Phys. Rev. Lett.* **98**, 106803 (2007).
- [42] L. Fu and C. L. Kane, Topological insulators with inversion symmetry, *Phys. Rev. B* **76**, 045302 (2007).
- [43] C. R. Ast, G. Wittich, P. Wahl, R. Vogelgesang, D. Pacilé, M. C. Falub, L. Moreschini, M. Papagno, M. Grioni, and K. Kern, Local detection of spin-orbit splitting by scanning tunneling spectroscopy, *Phys. Rev. B* **75**, 201401(R) (2007).